Article

A 6-month *in vivo* study of polymer/mesenchymal stem cell constructs for cranial defects

Halil Murat Aydin[1], Petek Korkusuz[2], İbrahim Vargel[3], Emine Kılıç[4], Elif Güzel[5], Tarık Çavuşoğlu[3], Duygu Uçgan[4] and Erhan Pişkin[1]

Abstract
Two biodegradable polymers, poly(L-lactide) and poly(ε-caprolactone) were blended (50/50) and used to produce polymeric scaffolds by the dual porogen approach using a salt leaching technique to create pores within the matrix, while supercritical-CO_2 treatment was used to enhance the interconnectivity and to remove impurities from synthesis steps. The scaffolds were highly porous (porosity $>$90%) with interconnected pore morphologies. These biodegradable scaffolds were evaluated in Sprague Dawley rats for osteoconductive properties over a 6-month period. Bone specimens were analyzed after 1, 3, and 6 months, for bone healing and tissue response. The cortical bone remodeling by controlled osteoblastic and osteoclastic activities as well as the bone marrow elements recovery were semi-quantitatively examined for each group. Excellent integration and biocompatibility behavior was observed in all groups. No adverse tissue responses were observed.

[1]Chemical Engineering Department and Bioengineering Division, Center for Bioengineering and Biyomedtek, Hacettepe University, Ankara, Turkey
[2]Department of Histology and Embryology, Faculty of Medicine, Hacettepe University, Ankara, Turkey
[3]Department of Plastics and Reconstructive Surgery, Faculty of Medicine, Kırıkkale University, Kırıkkale, Turkey
[4]Department of Pediatric Hematology – Bone Marrow Transplantation Unit and PEDI-STEM Stem Cell Research Centre Faculty of Medicine, Hacettepe University, Ankara, Turkey
[5]Department of Histology and Embryology, Cerrahpasa Faculty of Medicine, Istanbul University, Istanbul, Turkey

Corresponding author:
Erhan Pişkin, Chemical Engineering Department and Bioengineering Division, Center for Bioengineering and Biyomedtek, Hacettepe University, Ankara, Turkey
Email: piskin@hacettepe.edu.tr; erhanpiskin@biyomedtek.com

Introduction

Scaffolds made of polymers, ceramics, and composite materials have been used in tissue engineering for diverse applications. Usually, these materials meet some desirable properties, such as suitable mechanical strength, biocompatibility, and degradation.[1,2] Also, there are a number of fabrication procedures reported in the literature.[3–6] Basically, the aim of these methods is to enhance the surface area, interconnectivity, biocompatibility, and degradation.[7] As for the pore formation, one of the readily used methods is salt leaching in which controlled porosity can be achieved based on the leachable particles used.[8] Other approaches involve dual techniques which employ a second porogen to increase pore interconnectivity. In this study, we combine salt leaching and supercritical fluid treatment for porous matrix formation.

Defects in the cranium are a crucial problem. For example, critical size defects cannot be healed by the organism's intrinsic mechanisms; therefore, cranial defects have often been used to evaluate bone grafting and repair materials.[9–12] According to reported literature, Sprague Dawley rats fail to repair such defects.[13] Therefore, we used the same animal in our critical size cranial defect model to monitor the defect healing ability of materials that we developed in this study. Another requirement or approach for tissue engineering is to utilize differentiable cell lines, such as, stem cells. In this study, mesenchymal stem cells (MSCs) were used as they are found in a number of tissues, such as fat, trabecular bone, umbilical cord, and periosteum.[14] These cells are known to be multipotent and are able to differentiate into other cell lines like bone, cartilage, and muscle. Their differentiation activity can be triggered by inflammation and injury.[15–17]

This study investigates the ability of scaffolds with widely open and interconnected pores made of biodegradable polymeric blends of poly(L-lactide) (PLLA) and poly(ε-caprolactone) (PCL) with or without MSCs in the healing of critical size cranial defects in rats. For comparison, only MSCs were used in parallel studies. Although, the scaffold preparation, their pore structures, degradations, and mechanical properties are reported, we focused mostly on healing, new bone regeneration, and biocompatibility aspects in the animal models over a 6-month study.

Materials and methods

Biodegradable scaffolds

Biodegradable scaffolds, made of PLLA and PCL, were synthesized from the dimers and monomers under a nitrogen atmosphere for 30 and 4 h for PLLA and PCL, respectively, using 0.1% (w/w) Sn-2-ethylhexanoate catalyst ratio at 120°C. Detailed protocols for polymer synthesis and scaffold fabrication are reported in a previous study.[18] The polymers were characterized by nuclear magnetic resonance, Fourier transform infrared spectroscopy, and thermal analysis: gas permeation chromatography (GPC) (Shimadzu, Japan) was used to determine the average molecular weights of the polymers in chloroform at 25°C and 1 mL/min flow rate.

Biodegradable scaffolds were produced by applying two techniques: 'salt leaching' and supercritical carbon dioxide (scCO$_2$) treatment.'[18–20] Briefly, PLLA and PCL blends were prepared from their respective solutions (12% w/v) in a weight ratio of 50/50. These blends and NaCl crystals (Sigma, UK, with a 250–355 μm particle size) were mixed in a ratio of

1:11 and poured into a mold to obtain 8-mm diameter cylinders. The salt particles were extracted by deionized water.

The scaffolds were then treated with scCO$_2$ (at 2000 psi, 35°C) for 15 min to induce smaller pores on the pore walls. The pore structures were characterized by scanning electron microscopy (SEM; S 4500, Hitachi, Japan) and μ-CT (μCT 40, Scanco Medical AG, Brüttisellen, Switzerland) operated at 40 kVp and 180 μA.[20] The scaffolds with a diameter of 8 mm and a thickness of 1 mm were cut from the cylinders (∼2 cm long) produced in plastic syringes; therefore, both sides had the same pore morphology.

In order to determine *in vitro* degradation, the scaffolds ($n = 24$) were placed into glass vials and Ringer solution and antibiotics (1% v/v) was added. The vials were covered with cotton gauze and placed into a shaking water bath at 37°C and physiological pH (pH 7.4) for 6 months. During this test, four scaffolds were analyzed each month by GPC to determine the changes in the molecular weight and heterogeneity indices (HIs) of the materials.

The mechanical properties of the scaffolds (4 mm thick and 50.24 mm^2 surface area) ($n = 24$) were investigated using an Universal Test Instrument (Lloyd Instruments, LR5K Internal Extensometer, USA) in compression mode. The tests were conducted at room temperature using 500 N force and 10 mm/min rate according to ASTM D 695 standard. The elongation data were recorded against the compression strength. The Young's modulus was determined from the slope of the initial part of the strain–stress curves. Tests were repeated four times for each sample and mean values were recorded.

The animals were randomly divided into three groups (32×3) and treated as follows: (1) the scaffold group, scaffolds were only implanted in the cranial defects, (2) the scaffold–stem cell group, scaffolds were first implanted, then MSCs (1×10^6 cells per scaffold) were injected with a syringe into the pores of the scaffold, and (3) the stem cell group, no scaffolds, only stem cells (1×10^6 cells per cavity) were injected in the cavity of the cranial defects.

Stem cells

Femur and tibia allograft samples were obtained from the same species under general anesthesia and cultured in DMEM-LG solution (Sigma, Germany) containing 3% penicillin/streptomycin (Sigma, Germany). Under laminar flow, the femur and tibia samples were flushed with the incubation medium described below. The cells were then washed twice at 1500 rpm for 5 min. The cells (3×10^6 cells/cm^2) were incubated in 75-cm^2 Petri dishes in DMEM-LG (Sigma, Germany) medium containing 20% fetal bovine serum (FBS; Sigma, Germany), 1% penicillin/streptomycin, and 2 mM glutamine (Sigma, Germany) at 37°C and 5% CO$_2$. Media were changed every 3–4 days. Confluent cells were detached using 0.25% Trypsin/EDTA (Sigma, Germany) and cell count was calculated by using Tryphan blue. Counted cells were frozen in cell culture medium containing 10% dimethyl sulfoxide (Fluka, Germany) and kept in liquid nitrogen. For use in the animal experiments, cell pellets were re-suspended in phosphate-buffered saline with 1×10^6 cells per 50 μL and transferred to insulin injectors. Differentiation media composed of DMEM-LG, FBS, dexamethosone (Sigma, Germany), beta-glycerophosphate (Sigma, Germany), and ascorbic acid (Sigma, UK) was added to the cell culture plates including the stem cells and differentiation were monitored for 21 days. Osteogenic differentiation was confirmed by Alizarin Red staining.

Animal studies

The test animals, female Sprague Dawley rats ($n = 96$, weight: 200–330 g), were caged in a controlled environment (temperature: 22°C and 55% relative humidity) and food/water were administered *ad libitum* during the 6-month study. An alternating 12 h light and 12 h dark scheme was applied for 6 months. The protocol described below followed the mandate of the Hacettepe University – Animal Experiments Local Ethical Committee-Ethical Board (permission no: 2007/30-12 and date: March 26, 2007).

The animals were randomly divided into three groups (32×3) and treated as follows: (1) the scaffold group, scaffolds were only implanted in the cranial defects; (2) the scaffold–stem cell group, scaffolds were first implanted and then 1×10^6 MSCs 1×10^6 per scaffold were injected by syringe into the scaffold; and (3) the stem cell group, no scaffolds, only stem cells (1×10^6 cells per cavity) were injected in the cranial defects.

The animal weights were recorded and a sterile surgical procedure similar to that applied in other studies was used.[21,22] The animals were anesthetized with intraperitoneal ketamin HCl (Parke Davis, 50 mg/mL, Taiwan) and Rampun (2%) (Bayer, Germany) injections. The implantation site was shaved and disinfected with Batikon solution (Droksan, Turkey). Following iodide solution application, critical size defects of 8 mm in diameter were formed in the cranial area using a rotary, round-headed saw. The 'scaffolds,' 'scaffolds plus stem cells,' or 'stem cells' were immediately implanted into the cavities. During the animal studies, 32 animals were sacrificed; specimens were removed and placed in 10% phosphate-buffered formalin (pH 7.0) at room temperature for fixation. The samples were decalcified by immersion in De Castro solution for 5–10 days before dehydration. They were rinsed in buffer, dehydrated in a graded series of ethanol, and then embedded in paraffin. Five micrometer-thick serial sections were cut with a microtome (Leica, Germany). Haematoxylin & Eosin and Masson's trichrome.

The sections were stained and evaluated for defect healing, new bone formation, and tissue response to cells and/or implant. Two independent investigators evaluated the bone graft sections using Leica DMR microscope with a DC500 digital camera (Germany) and quantitatively analyzed with a Leica Qwin Plus computer image analysis system (Germany). One section from every 20 sections was randomly taken and quantified. The new bone area in the defect was calculated based on Masson's trichrome-stained sections. The defect healing and implant biocompatibility (tissue response) were semi-quantitatively scored. Statistical tests were applied to evaluate the histology parameters. The normality of distribution and the homogeneity of variances of the sample were established using the Shapiro–Wilk test.

The quantity of new bone was analyzed by parametric variance analysis tests (one-way ANOVA and Tukey's test for multiple comparison and as *post hoc* test, respectively) to assess statistical significance. Bone healing and tissue response were analyzed by non-parametric tests (Kruskal–Wallis for multiple comparison and Mann Whitney *U* as *post hoc* test with Bonferoni correction). Descriptive statistical values were expressed as mean, standard deviation, minimum, and maximum.[23]

Results and discussion

Scaffolds

PLLA and PCL were synthesized by homopolymerization of the respective dimer and monomer at predetermined conditions and 50/50 (w/w) PLLA/PCL blends were used to

prepare porous scaffolds in cylindrical forms by molding, salt leaching, and $scCO_2$ treatment.[19,20] The properties of the polymers and scaffolds produced in this study are summarized in Table 1.

A representative μ-CT image of the scaffolds made of PLLA/PCL blends is given in Figure 1. The scaffolds were highly porous structures (porosities up to 94.7%; analyzed by μ-CT) as a result of the salt leaching technique. The $scCO_2$ treatment caused the formation of extra but smaller pores especially on the pore walls that increased the interconnectivity within the porous scaffold matrix significantly. The polymer content in the scaffolds was only ∼5% of the total volume, this is a very significant property for scaffolds in tissue engineering and occupied only 1/20 of the defect volume.

The number and weight average molecular weights of the blend decreased to about 56,000 and 22,000, respectively, after 6 months (almost half of the initial values; Table 1) when the scaffolds were degraded in Ringer's solutions. HI was 2.9 after 1 month and only decreased to 2.6 in 6 months. The decrease in the molecular weight is reasonable since full bone regeneration takes about a year or more; therefore, supporting the newly forming tissues with the help of scaffold by physical means is important, and could be critical.[18]

According to the mechanical test data obtained from the four individual measurements, the Young's modulus of the scaffolds was 31.15 ± 1.43 kPa. This value was expected for a highly porous material (>90%), but is sufficient for non-load-bearing applications.

Calvarial bone healing (histological evaluation)

The implantation procedure is shown in Figure 2. These porous biodegradable polymeric scaffolds, made of PLLA and PCL blends alone and/or combined with MSCs, were

Table 1. Physical properties of the polymers and scaffolds

| Properties	
Weight average molecular weight (M_w) and HI of PLLA used for the scaffolds (kDa)[a]	∼200/2.44
Weight average molecular weight (M_w) and HI of PCL used for the scaffolds (kDa)[a]	∼40/1.78
The PLLA/PCL weight ratio in the blends used for the scaffolds	50/50
Scaffold shape/diameter (mm)/thickness (mm)	Cylindrical/8/1
Scaffold porosity (%)[b]	94.7 ± 0.4
Scaffold pore size range (μm)	250–355
Scaffold pore thickness (mm)[b]	0.21 ± 0.01
Scaffold pore interconnectivity (1)[b]	538.1 ± 16.4
Unit scaffold surface (1/mm)[b]	8.3 ± 0.01
Scaffold degradation in Ringer solution[a]	
The weight average molecular weight of the blend after 1/3/6 months	109,077/86,044/56,337
The HI of the blend after 1/3/6 months[d]	2.92/2.74/2.60
Young's modulus (kPa)[c]	31.15 ± 1.43
EtO sterilization at 37°C (h)	24

[a]Determined by GPC.
[b]Determined by μ-CT.
[c]Determined by Universal Test Instrument.
[d]Average of four scaffolds.

evaluated for their restoration capabilities in critical-size cranial defects induced in Sprague Dawley rats. Only stem cells as the third group of animal tests were used for comparison. The materials were placed into the cranial defects and the defect area of the test animals were examined macroscopically (Figure 3) after the 1, 3, and 6 months. We did not observe any foreign body reaction with fibrosis, necrosis, and/or scar tissue formation in none of the animal groups during the 6 months. Even though the surgical operation was quite severe and the implants quite large (8 mm in diameter and 1 mm thick), there were no animal deaths during the test period. It should be noted that the polymer used was a blend of two well-known biodegradable polymers, PLLA and PCL, and the percentage of the polymer phase was only about 5% of the total volume due to the high porosity of the scaffolds prepared for this study.
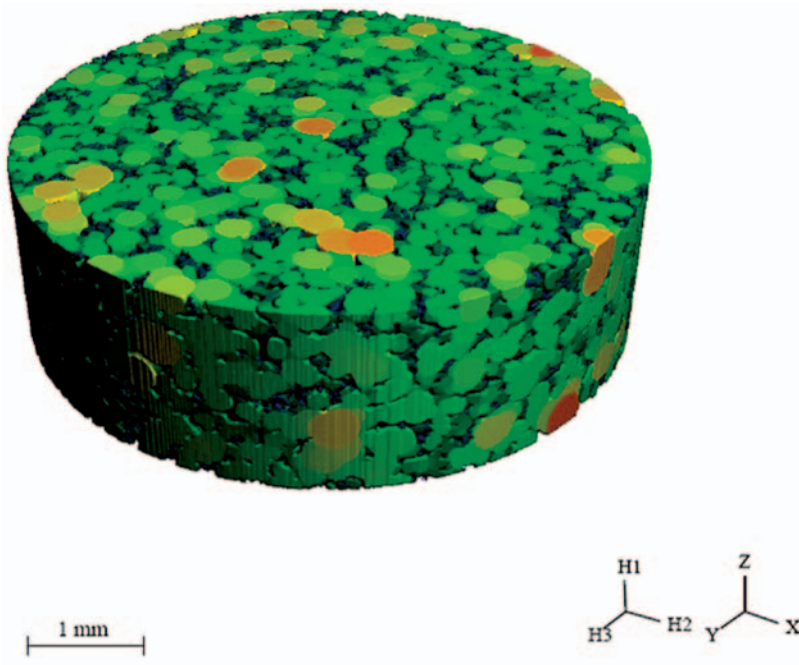
Figure 1. A representative μ-CT image of the PLLA/PCL blend scaffolds

Figure 2. Animal surgical procedure: (a) cranial defect created and scaffold before implantation; (b) scaffold implanted into the cranial defect; and (c) introducing stem cells within the cavities of the implanted scaffold

Following macroscopic examination, the bone specimens were taken from the defect areas (including the surrounding tissue) and histologically examined for bone repair and tissue responses. The scoring techniques applied and the results are given in Table 2. Shown in Figures 4–6 are representative histological images of the samples taken after 1, 3, and 6 months, respectively, at two different magnifications for the 'scaffold,' 'stem cell,' and 'scaffold–stem cell' groups.

The quantitative and qualitative histological analyses of the bone healing revealed that the critical size cavity was not totally ossified at the end of 6 months in any of the groups; this has also been reported in similar studies.[24,22] However, very positive/promising healing processes without any significant tissue reactions were observed as summarized and discussed below.

Bone defect healing

Listed in Table 3 are the bone defect healing scores and the tissue responses to the implants. The bone defect healing scores increased significantly in all groups from day 30 to 180. Defect healing scores increased significantly from 30 to 90 days and from 30 to 180 days in all groups ($p < 0.005$).

The descriptive statistics regarding new bone area measurements (μm^2) are given in Figure 7. The 3-month new bone formation rate was significantly higher than that after 1 month in the scaffold group ($p = 0.00$); but there was no significant difference for the stem cell and scaffold–stem cell-implanted groups. The 6-month new bone formation measurements were also significantly higher than that after 1 month in all groups ($p = 0.00$). The new bone formation (green-stained bone area in the images) was significantly greater in the scaffold–stem cell group compared to that of the scaffold group after months 1 and 3 ($p = 0.00$ and $p = 0.004$, respectively). The stem cell group received significantly higher scores for new bone formation compared

Figure 3. A sample image showing the defect site at the end of 3 months in the scaffold–stem cell group

Table 2. Histological scoring system summary (Bone defect repair and the tissue response are scored separately)

Categories	Parameters	Scores			
Category I		3	2	1	0
Bone defect repair	New bone formation in the defect	Full bone formation in the defect	Moderate bone formation (>50%)	Mild bone formation (<50%)	No new bone
	Graft resorption	Full resorption	Moderate resorption (>50%)	Mild resorption (<50%)	No resorption
	Marrow changes	Adult-type fatty marrow	>50% replaced by new tissue	<50% replaced by new tissue	Fibrous tissue or red
	Cortex remodeling	Full remodeling cortex	Moderate remodeling (>50%)	Mild remodeling (<50%)	No remodeling

Categories	Parameters	Scores				
Category 2		4	3	2	1	0
Tissue response	Fibrous connective tissue formation	Severe deposition of dense collagenous connective tissue around implant	Disruption of normal tissue architecture and presence of moderately dense fibrous connective tissue	Presence of moderate connective tissue	Presence of delicate spindle-shaped cells or mild fibroplasia	No difference from normal control tissue, absence of connective tissue at or around implant site
	Inflammatory cellular infiltration	Severe cellular infiltrate response to implant or tissue necrosis at or around the site	Presence of large numbers of lymphocytes, macrophages, and foreign body giant cells, also notable presence of eosinophils and neutrophils	Presence of several lymphocytes, macrophages with a few foreign body giant cells, and a small foci of neutrophils	Presence of a few lymphocytes or macrophages, no presence of foreign body giant cells, eosinophils, or neutrophils	No difference from normal control tissue, no presence of macrophages, foreign body cells, lymphocytes, eosinophils, or neutrophils at or around implant site
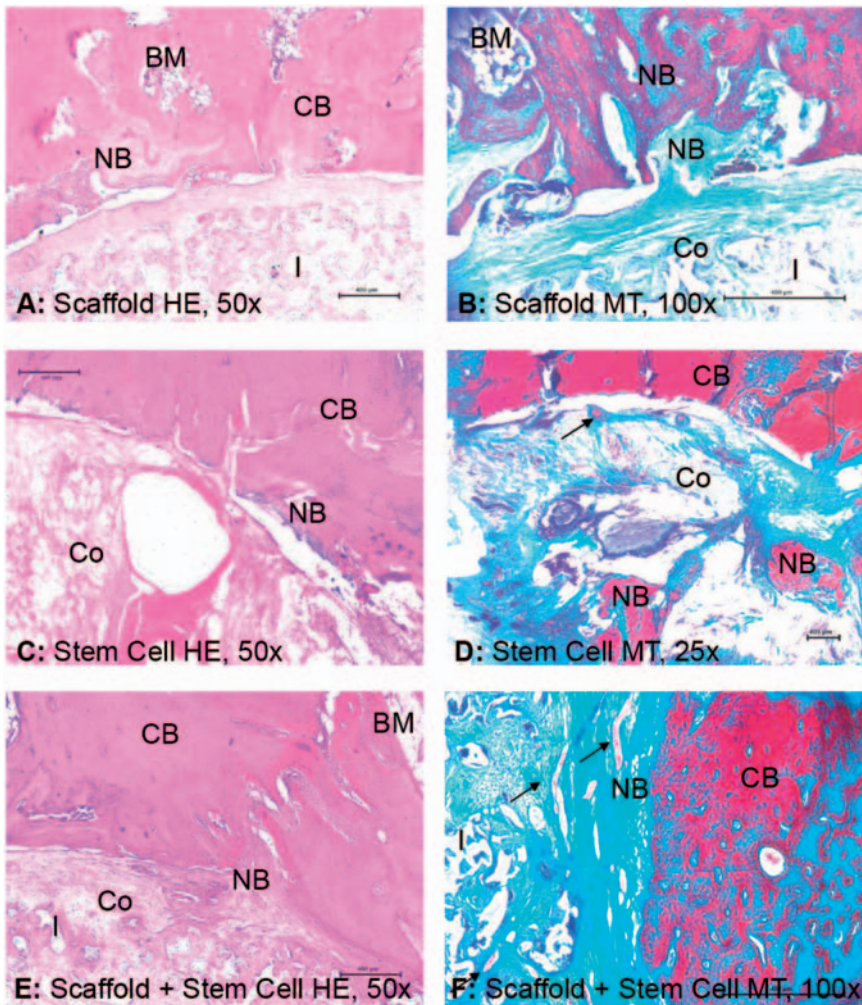
Figure 4. After 1 month: Ossification started from cortical bone edges within the defect area (a)–(f). Defect healing process is at more advanced level in stem cell group (c and d) and scaffold–stem cell (e and f) group comparing to that of the scaffold samples (a and b). Collagen fibers (pink with HE; green with MT) and the blood vessels (arrow) are located, in close relation with the dissolving implant particles; showing the biocompatibility and the good guidance for the polymer. Note that bony spicules guiding the ossification are present within the cavity in D.   Note: HE, hematoxylin eosin; MT, Masson's trichrome; I, implant; CT, connective tissue; BM, bone marrow; CB, compact bone; NB, new bone; and Co, collagen fibers

to the scaffold group ($p = 0.06$) after month 1; but the difference was not significant after 3 months.

There was no statistically significant difference between the stem cell and scaffold–stem cell groups regarding new bone formation after months 1 and 3. There was no statistically significant difference seen between groups for new bone formation in or after month 6 (Figure 7).
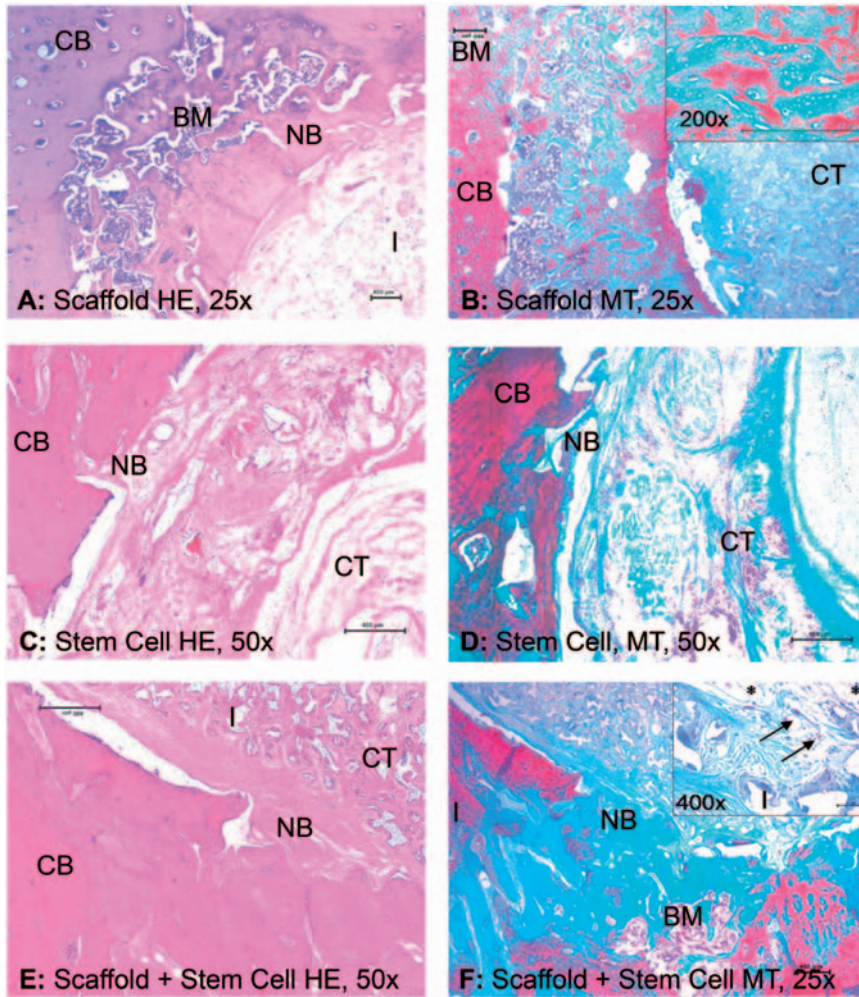
Figure 5. After 3 months: The green new bone layer (osteoid) at the cortical edges is thicker than day 30 in all groups. Maturing bone matrix undergoing Haversian remodeling in red-green with MT is seen at inset (b). The cavity is filled with a disorganized loose connective tissue in (c) and (d). Dissolving polymeric particles adjacent to vessels and tiny collagen fibers fill the cavity in the scaffold implanted groups (a, b, e, and f). Note the presence of collagen fibers (green with MT), macrophages (arrows) and the small blood vessels (stars) adjacent to the polymer particles in inset F.   Note: HE, haematoxylin eosin; MT, Masson's trichrome; I, implant; CT, connective tissue; BM, bone marrow; CB, compact bone; and NB, new bone

Cortical bone remodeling by controlled osteoblastic and osteoclastic activities and the bone marrow elements recovery were semi-quantitatively examined for each group. The ossification process started from the edges of the cortical bone and went toward the center in the scaffold and stem cell groups (Figures 4–6). A fibrous capsule surrounded the polymer particles in all groups. These particles stimulated new bone formation by guiding new small blood vessels within these thin collagenous capsules (Figures 4(a), (b), (e), and (f); 5(a), (b), (e), and (f); and 6(a), (b), (e), and (f)). The stem cell group gave better results
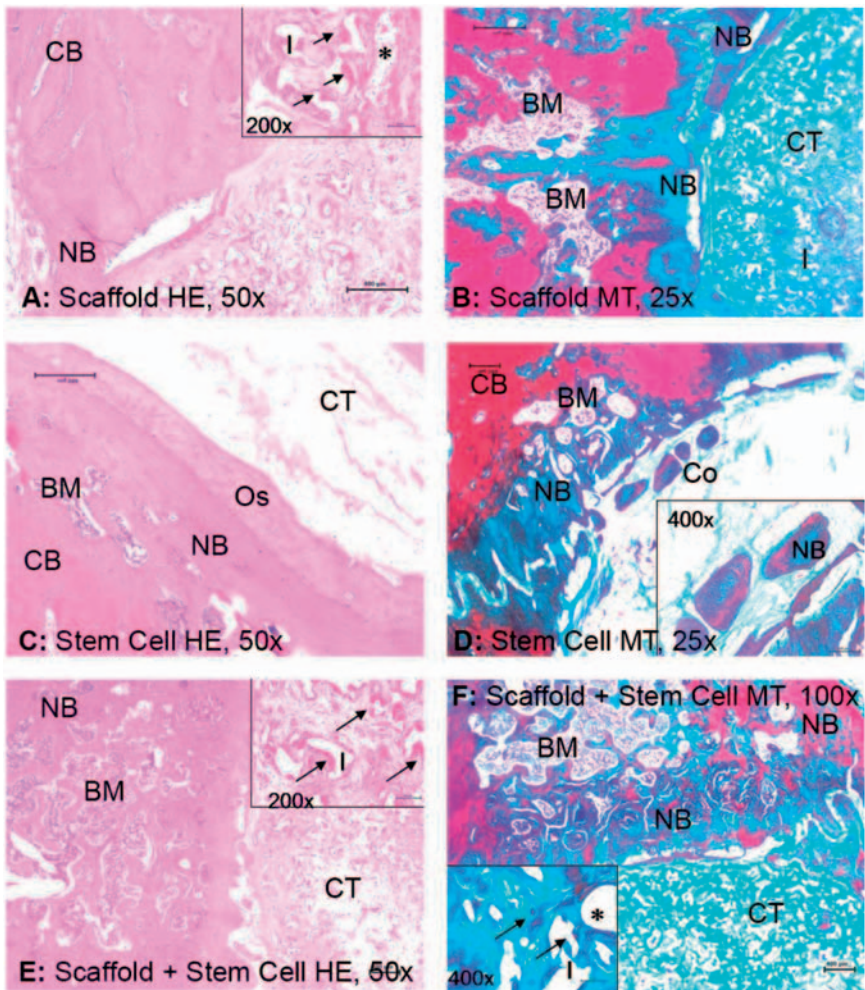
Figure 6. After 6 months: Although new bone layer is significantly thicker compared to previous time points, critical size defect is still filled with fibrous callus in all groups (a)–(f). Stem cell applied cavity remains to be filled with a disorganized loose connective tissue (c and d). However, the healing process is accelerated with the presence of a thick new bone layer (note the two distinct new bone layer marked by Os and NB in (c)) and ossifying small bony spicules within the cavity in this group (d inset). Polymer is degrading from the periphery toward inside and dividing particles and/or porosities make compartments that are surrounded by thin capsules containing macrophages, epitheloid giant cells (arrows) and fibroblasts (insets of a, e, and f). Remodeling of new bone layer and bone marrow recovery is better in cell-scaffold applied groups (e, f) when compared to others. Note: HE, hematoxylin eosin; MT, Masson's trichrome; I, implant; CT, connective tissue; BM, bone marrow; CB, compact bone; NB, new bone; and Star, blood vessel

regarding the marrow recovery and new bone remodeling compared to the scaffold groups after 6 months (Figure 6(a)–(f)). The marrow cavity was filled with hematopoietic precursor cells and the fat islands in this group. But the difference was not statistically significant regarding total bone defect healing score. Ma et al.[25,26] reported promising results with

Table 3. Descriptive statistics

| Parameter	Time (month)	Group	N	Arithmetic mean	Standard deviation	Median	Minimum	Maximum
Bone defect repair	1	'Scaffold'	10	2.4167	0.51493	2.000	2.00	3.00
		'Stem cell'	10	3.2000	0.63246	3.000	2.00	4.00
		'Scaffold–stem cell'	10	3.0833	0.51493	3.000	2.00	4.00
	3	'Scaffold'	10	3.1667	0.57735	3.000	2.00	4.00
		'Stem cell'	10	4.0000	0.57735	4.000	3.00	5.00
		'Scaffold–stem cell'	10	4.3333	0.65134	4.000	3.00	5.00
	6	'Scaffold'	12	3.7500	0.75308	4.000	3.00	5.00
		'Stem cell'	12	4.0000	0.86603	4.000	3.00	5.00
		'Scaffold–stem cell'	12	4.5000	0.67420	5.000	3.00	5.00
Tissue Response	1	'Scaffold'	10	2.4167	0.51493	2.000	2.00	3.00
		'Stem cell'	10	1.0000	0.00000	1.000	1.00	1.00
		'Scaffold–stem cell'	10	2.2727	0.46710	2.000	2.00	3.00
	3	'Scaffold'	10	2.3333	0.49237	2.000	2.00	3.00
		'Stem cell'	10	1.0000	0.00000	1.000	1.00	1.00
		'Scaffold–stem cell'	10	2.2500	0.45227	2.000	2.00	3.00
	6	'Scaffold'	12	2.3333	0.49237	2.000	2.00	3.00
		'Stem cell'	12	1.0000	0.00000	1.000	1.00	1.00
		'Scaffold–stem cell'	12	2.4167	0.51493	2.000	2.00	3.00

Tissue response and defect healing scores are the variables. The data of variables belonging to different groups are given as mean, minimum, maximum, medium, and standard deviation values.

polymer/ceramic/collagen composites as posterolateral and intervertebral spinal fusion materials. Other groups also suggested the use of scaffold/cell constructs for bone repair.[27–29] Zhou et al. reported that PLLA-nano hydroxyapatite scaffolds combined with MSCs can enhance and accelerate bone formation.[30]

The stem cell group revealed the best cortical bone remodeling and new bone formation in the defect area at the end of 1 month (Figure 4(c) and (d)). Disorganized ossifiying bony islands and accelerated healing (almost equal to the scaffold–stem cell group) were observed within the defect in this group after 2 months (Figure 5(c) and (d)); but healing process was not promoted after 6 months compared to the other groups (Figure 6(c) and (d)). On the other hand, the stem cell group did not have significantly higher total bone defect healing scores compared to other groups.

Tissue response

Tissue response scores remained low and did not significantly differ between groups and by time (Table 3). Neither fibrosis (scar tissue), necrosis, nor foreign body reaction was noted in any of the samples at any time point. The polymeric scaffolds caused mild to moderate
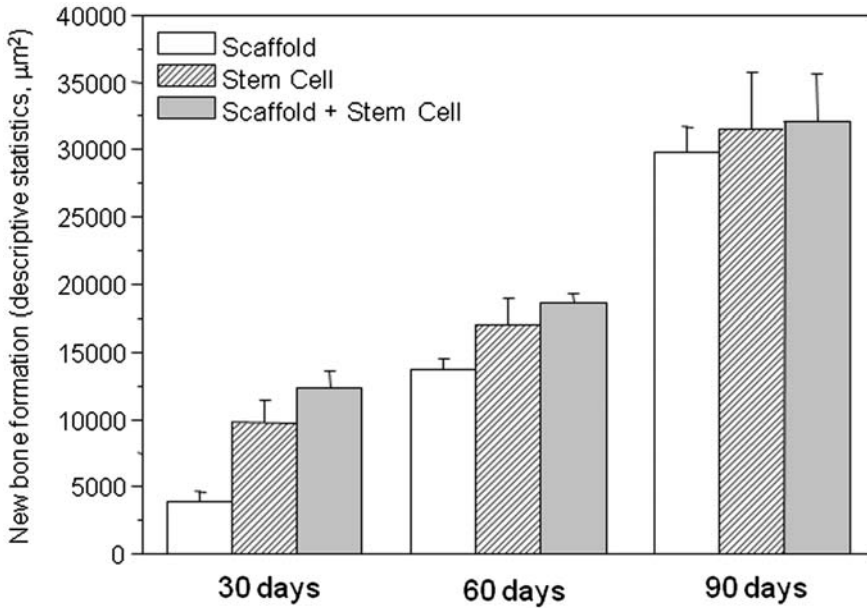
Figure 7. Descriptive statistics regarding to new bone area measurement (μm^2)

inflammation that was characterized mainly by mononuclear phagocytic cells, macrophages, lymphocytes, and fibroblasts. Some scattered polymorphonuclear leukocytes with foreign body giant cells were also noted (insets of Figure 6(a), (e), and (f)).

A highly vascular and cellular connective tissue was observed surrounding the polymer particles within the cavity initiated the intra membrane formation of new bone capsules in the scaffold and scaffold–stem cell implanted groups. The capsule was more cellular and vascular; the newly formed bone trabecules were greater in the scaffold–stem cell group compared to the scaffold group (Figure 4). Degradation of the polymer started from the periphery at 1 month. However, polymer particle residues were still intact at 6 months (Figures 4(a), (b), (e), and (f); 5(a), (b), (e), and (f); and 6(a), (b), (e), and (f)).

Conclusions

In this study, we reported the use of highly porous biodegradable scaffolds with or without stem cells for repairing critical size cranial defects in a rat model. Both salt leaching and $scCO_2$ treatment were used to obtain the highly open pore structures with very high interconnectivity between the pores. The $scCO_2$ application not only produced extra small pores on the pore walls which increased the interconnectivity, but also allowed removal of residuals within the scaffolds and eliminated the potential side effects in *in vivo*. The porosity of the scaffolds was over 90% with less than 10% polymer in the scaffolds; this is a very important property if one considers the possible side effects of the polymers and their degradation products. Degradation data imply that the weight of the polymeric blend was halved after 6 months which means less than 5% of the cavity volume was occupied by polymer at that time; consequently, the scaffold was still able to support the newly forming tissue.

There were no foreign body reactions, such as fibrosis, necrosis, or scar tissue formation in any of the groups and no animals died during the 6-month experiment. The cranial defect healing and new bone formation of all three groups, the 'scaffolds,' 'scaffold-stem cells' and 'stem cells,' were very similar. It is felt that supporting the defect area mechanically for more than 6 months may lead even better bone formation; therefore, the 'scaffold–stem cells group' may be the more effective repair strategy.

Acknowledgements

References

1. Freed LE, Vunjak-Novakovic G, Biron RJ, et al. Biodegradable polymer scaffolds for tissue engineering. *Biotechnology* 1994; 12: 689–693.

2. Hutmacher DW. Scaffolds in tissue engineering bone and cartilage. *Biomaterials* 2000; 21: 2529–2543.

3. Tai H, Mather ML, Howard D, et al. Control of pore size and structure of tissue engineering scaffolds produced by supercritical fluid processing. *Eur Cell Mater* 2007; 14: 64–77.

4. Ko YG, Kawazoe N, Tateishi T and Chen G. Preparation of novel collagen scaffolds using an ice particulate template. *J Bioact Compat Polym* 2010; 25: 360–373.

5. Lebourg M, Sabater Serra R, Más Estellés J, Hernández Sánchez F, Gómez Ribelles JL and Suay Antón J. Biodegradable polycaprolactone scaffold with controlled porosity obtained by modified particle-leaching technique. *J Mater Sci Mater Med* 2008; 19(5): 2047–2053.

6. Hou Q, Grijpma DW and Feijen J. Porous polymeric structures for tissue engineering prepared by a coagulation, compression moulding and salt leaching technique. *Biomaterials* 2003; 24(11): 1937–1947.

7. Ranucci CS, Kumar A, Batra SP and Moghe PV. Control of hepatocyte function on collagen foams: sizing matrix pores toward selective induction of 2-D and 3-D cellular morphogenesis. *Biomaterials* 2000; 21: 783–793.

8. Thomson RC, Yaszemski MJ, Powers JM and Mikos AG. Fabrication of biodegradable polymer scaffolds to engineer trabecular bone. *J Biomater Sci Polym Ed* 1995; 7: 23–38.

9. Mulliken JB and Glowacki J. Induced osteogenesis for repair and construction in the craniofacial region. *Plast Reconstr Surg* 1980; 65(5): 553–560.

10. Aalami OO, Nacamuli RP, Lenton KA, et al. Applications of a mouse model of calvarial healing: differences in regenerative abilities of juveniles and adults. *Plast Reconstr Surg* 2004; 114(3): 713–720.

11. Hollinger JO and Kleinschmidt JC. The critical size defect as an experimental model to test bone repair materials. *J Craniofac Surg* 1990; 1(1): 60–68.

12. Schmitz JP and Hollinger JO. The critical size defect as an experimental model for craniomandibulofacial nonunions. *Clin Orthop Relat Res* 1986; 205: 299–308.

13. Montjovent MO, Mathieu L, Schmoekel H, et al. Repair of critical size defects in the rat cranium using ceramicreinforced PLA scaffolds obtained by supercritical gas foaming. *J Biomed Mater Res Part A* 2007; 83(1): 41–51.

14. Bianco P and Riminucci M. The bone marrow stroma in vivo: ontogeny, structure, cellular composition and changes in disease. In: Beresford JN and Cambridge ME (eds) *Marrow stromal cell culture: handbooks in practical animal cell biology*. Cambridge: Cambridge University Press, 1998, pp. 10–25.

15. Ngiam M, Liao S, TOJ Jie, et al. Effects of mechanical stimulation in osteogenic differentiation of bone marrow-derived mesenchymal stem cells on aligned nanofibrous scaffolds. *J Bioact Compat Polym* 2011; 26: 56–70.

16. Lou J, Xu F, Merkel K and Manske P. Gene therapy: adenovirus-mediated human bone

morphogenetic protein-2 gene transfer induces mesenchymal progenitor cell proliferation and differentiation in vitro and bone formation in vivo. *J Orthop Res* 1999; 17: 43–50.

17. Dånmark S, Finne-Wistrand A, Wendel M, Arvidson K, Albertsson A-C and Mustafa K. Osteogenic differentiation by rat bone marrow stromal cells on customized biodegradable polymer scaffolds. *J Bioact Compat Polym* 2010; 25: 207–223.

18. Duarte AR, Mano JF and Reis RL. Perspectives on: supercritical fluid technology for 3D tissue engineering scaffold applications. *J Bioact Compat Polym* 2009; 24: 385–400.

19. Aydin HM, El Haj AJ, Pişkin E and Yang Y. Enhancing pore interconnectivity in polymeric scaffolds for tissue engineering. *J Tissue Eng Regen Med* 2009; 3(6): 470–476.

20. Aydin HM, Yang Y, Kohler T, El Haj A, Müller R and Pişkin E. Interaction of osteoblasts with macroporous scaffolds made of PLLA/PCL blends modified with collagen and hydroxyapatite. *Adv Eng Mater* 2009; 11(8): B83–B88.

21. Xie LN, Wang P, Pan JL, Sun Z and Cui FZ. The effect of platelet-rich plasma with mineralized collagen-based scaffold on mandible defect repair in rabbits. *J Bioact Compat Polym* 2010; 25: 603–621.

22. Lu M and Rabie ABM. Quantitative assessment of early healing of intramembranous and endochondral autogenous bone grafts using micro-computed tomography and Qwin image analyzer. *Int J Oral Maxillofac Surg* 2004; 3: 369–376.

23. Montjovent MO, Mark S, Mathieu L, et al. Human fetal bone cells associated with ceramic

reinforced PLA scaffolds for tissue engineering. *Bone* 2008; 42: 554–564.

24. Montjovent MO, Mathieu L, Schmoekel H, et al. Repair of critical size defects in the rat cranium using ceramic-reinforced PLA scaffolds obtained by supercritical gas foaming. *J Biomed Mater Res* 2007; 83A: 41–51.

25. Ma X, Wu X, Wu Y, et al. Posterolateral spinal fusion in rabbits using a RP-based PLGA/TCP/Col/BMSCs-OB biomimetic grafting material. *J Bioact Comp Polym* 2009; 24(5): 457–472.

26. Ma X, Wu X, Hu Y, et al. Intervertebral spinal fusion using a RP-based PLGA/TCP/bBMP biomimetic grafting material. *J Bioact Comp Polym* 2009; 24(1 Suppl): 146–157.

27. Wilmonsky CV, Lutz R, Meisel U, et al. In vivo evaluation of ß-TCP containing 3D laser sintered poly(ether ether ketone) composites in pigs. *J Bioact Comp Polym* 2009; 24(2): 169–184.

28. Kyriakidou K, Lucarini G, Zizzi A, et al. Dynamic co-seeding of osteoblast and endothelial cells on 3D polycaprolactone scaffolds for enhanced bone tissue engineering. *J Bioact Comp Polym* 2009; 23(3): 227–243.

29. Li H, Zheng Q, Xiao Y, Feng J, Shi Z and Pan Z. Rat cartilage repair using nanophase PLGA/HA composite and mesenchymal stem cells. *J Bioact Comp Polym* 2009; 24(1): 83–99.

30. Dong JL, Li LX, Mu WD, et al. Bone regeneration with BMP-2 gene-modified mesenchymal stem cells seeded on nano-hydroxyapatite/Collagen/poly(L-lactic acid) scaffolds. *J Bioact Compat Polym* 25: 547–566.